American Mineralogist, Volume 84, pages 933–936, 1999

Al-Fe disorder in synthetic epidotes: A single-crystal X-ray diffraction study

GABRIELE GIULI, PAOLA BONAZZI, AND SILVIO MENCHETTI*

Dipartimento di Scienze della Terra, Università di Firenze, Via G. la Pira 4, 50121 Firenze, Italy

ABSTRACT

Synthetic epidotes were produced using a Tuttle type hydrothermal vessel in the temperature range from 500 to 700 °C and at 4.5 to 5.0 kbars pressure. Single-crystal X-ray diffraction structure refinements yielded intracrystalline cation distributions for two crystals grown at 600 °C (0.68 and 0.73 Fe apfu) and five crystals grown at 700 °C (0.88 to 1.08 Fe apfu). The resulting Fe occupancies were compared with those calculated according to a thermodynamic model: The samples formed at 700 °C display a Fe distribution between M3 and M1 sites that match the calculation; nevertheless, we found the presence of a small but appreciable amount of Fe in the M2 sites that increases with the total Fe content (up to 0.08 Fe apfu). The crystals formed at 600 °C show a much higher disorder than expected, but have no Fe in the M2 site. Crystal-chemical features of the samples studied were compared with those of a previously published set of natural epidotes displaying a much lower Fe disorder: In particular, the unit-cell volume vs. Fe content relationship is not affected by the intracrystalline Fe distribution. This relation suggests that the Al-Fe intracrystalline distribution is independent of pressure.

INTRODUCTION

Epidotes are common rock-forming minerals with the ideal composition $Ca_2Al_{3-X}Fe_X[SiO_4][Si_2O_7]O(OH)$. Their structure consists of edge-sharing octahedral chains parallel to the **b** axis, connected by SiO_4 and Si_2O_7 groups. Large cavities (A1 and A2) exist in which Ca cations are located. Three nonequivalent octahedral sites are present in the structure: M1 octahedra form branched chains with M3 octahedra alternately attached on opposite sides, whereas M2 octahedra form single chains. M3 is the largest and most distorted site, M2 the smallest and most regular. Fe is preferentially located in the M3 site and enters the M1 site to a lesser extent; the M2 site is usually occupied solely by Al.

Bird and Helgeson (1980) developed a theoretical model to relate temperature and Fe intracrystalline distribution on the basis of experimental phase-equilibrium data for epidotes (Holdaway 1972; Liou 1973), Fe occupancies determined by Mössbauer spectroscopy on synthetic samples (Dollase 1973), and the thermodynamic properties of CO_2-H_2O fluids and coexisting phases. According to this model, Fe located at M1 increases with temperature and total Fe content.

Application of this model to the study of hydrothermal epidotes in natural systems yielded substantial disagreement with both the actual temperatures at the sampling sites (Bird et al. 1988) and with estimated paleotemperatures (Patrier et al. 1991). Both papers claimed a metastably higher disorder for some of the samples examined. In particular, Bird et al. (1988) found that an epidote sample from the biotite zone displayed a Fe distribution corresponding to 390 °C that was in agreement with the probable downhole temperature of 340 °C, whereas three other samples from the chlorite+calcite zone (probable downhole temperatures from 265 to 300 °C ca.) displayed Fe occupancies corresponding to 450–600 °C. Patrier et al. (1991) found that the discrepancy between the observed and calculated intracrystalline Fe distribution was closely related to the distance from the thermal source, and that rapid crystal growth was not sufficient to explain the metastable state of Fe disordering. Recently, Fe occupancies determined by Mössbauer spectroscopy on heat-treated natural epidotes (Fehr and Heuss-Assbichler 1997) indicate much lower disorders than those predicted from the model of Bird and Helgeson (1980). Two possible reasons could account for this discrepancy: (1) the Mössbauer analysis carried out on the synthetic samples (Dollase 1973) may not be reliable because of the simultaneous presence of different Fe-bearing phases in the run products or (2) the synthetic epidotes themselves may be metastably disordered (Fehr and Heuss-Assbichler 1997).

The present study aims to obtain more experimental data on the Fe intracrystalline distribution as a function of temperature. To avoid dealing with the kinetics of disordering, the synthetic crystals studied were rapidly cooled to room temperature. Despite the inherent difficulties, we were able to synthesize suitable crystals to perform single-crystal X-ray diffraction study.

EXPERIMENTAL METHODS

Syntheses were performed using a Tuttle type hydrothermal apparatus at temperatures and pressures ranging from 500 to 700 °C and from 4.5 to 5.0 kbar. The oxygen fugacity was controlled using a Cu-Cu_2O buffer according to the technique described by Eugster and Wones (1962). More details about the syntheses and their results are given elsewhere (Giuli et al. in preparation).

Seven crystals were selected for intensity data collection on the basis of their optical homogeneity and diffraction quality.

*E-mail: crystal@cesit1.unifi.it

Difficulties in finding suitable crystals arose from the fact that the great majority of them were found to be twinned and their dimensions were small. Unit-cell parameters (Table 1) were measured using a CAD4 single crystal diffractometer and Mo*K*a radiation monochromatized by a graphite crystal. The intensities of the equivalent monoclinic reflections *hkl* and $h\bar{k}l$ were collected as described in Table 2 and subsequently corrected for Lorentz-polarization. Absorption was corrected according to the semiempirical method of North et al. (1968). Structure refinements were performed using the program SHELX76 (Sheldrick 1976). We used the same refinement strategy as Bonazzi and Menchetti (1995) to obtain the best reproducibility when comparing the results of the two works. The relevant data of the refinements are summarized in Table 3. The F_{obs}–F_{calc} list is reported in Table 4a[1], and the atomic coordinates together with anisotropic displacements are given in Table 4b[1]. Chemical composition of the crystals studied (Table 5) was determined by a JEOL JXA 8600 electron microprobe operating at 15.0 kV and 10.0 nA. Data were corrected using the Bence and Albee (1968) algorithm.

[1]For a copy of Table 4a and Table 4b, document item AM-99-011, contact the Business Office of the Mineralogical Society of America (see inside front cover of recent issue) for price information. Deposit items may also be available on the American Mineralogist web site at http://www.minsocam.org.

TABLE 1. Unit cell dimensions together with their standard deviations

Sample	*a* (Å)	*b* (Å)	*c* (Å)	β (°)	*V* (Å3)
CC11c	8.891(2)	5.624(2)	10.164(2)	115.44(2)	458.9(2)
CC11b	8.890(2)	5.628(1)	10.161(3)	115.42(2)	459.2(2)
CC9e	8.894(2)	5.636(1)	10.162(2)	115.40(2)	460.2(2)
CC16b	8.887(3)	5.625(2)	10.161(2)	115.40(2)	458.8(3)
CC20c	8.902(3)	5.640(1)	10.174(1)	115.41(2)	461.4(2)
CC12a	8.900(2)	5.650(2)	10.170(2)	115.40(2)	462.0(2)
CC13a	8.903(2)	5.651(1)	10.171(2)	115.39(1)	462.3(2)

TABLE 2. Experimental conditions for intensity data collection

Sample	ϑ_{min}–ϑ_{max} (°)	scan speed (°/min)	scan mode	scan width (°)	crystal dimensions (mm × mm × mm)
CC11c	2–32	1.4	ω	3.0	10 × 20 × 120
CC11b	2–32	1.8	ω	2.5	15 × 30 × 90
CC9e	2–32	1.8	ω	2.5	20 × 70 × 90
CC16b	2–32	0.7	ω	2.5	10 × 60 × 80
CC20c	2–32	0.8 - 8.2	ω	2.6	20 × 50 × 100
CC12a	2–32	1.4	ω	2.8	20 × 60 × 120
CC13a	2–32	1.8	ω	2.8	30 × 60 × 120

TABLE 3. Refinement statistics

	R_{symm} (%)	R_{obs} (%)	R_w (%)	*S*	Ni*	N_o†	Nr‡
CC11c	8.23	4.12	3.07	2.62	1505	660	62
CC11b	3.03	3.59	2.78	1.50	1637	883	124
CC9e	3.64	3.71	2.88	1.34	1604	811	124
CC16b	4.61	4.49	3.99	1.78	1675	1050	124
CC20c	5.88	3.90	3.70	1.30	1515	714	118
CC12a	4.54	4.42	3.51	1.65	1610	691	109
CC13a	2.36	2.89	2.32	1.56	1669	1058	124

* Number of unique reflections.
† Number of observed reflections [$F_o > 8\sigma(F_o)$].
‡ Number of refined parameters.

TABLE 5. Chemical compositions (wt%) and atomic proportions† of the crystals studied

	CC11c	CC11b	CC9e	CC16b	CC12a	CC13a
SiO_2	37.77	38.30	37.16	38.45	37.05	37.49
Al_2O_3	24.66	24.74	22.64	23.21	19.75	20.71
Fe_2O_3	10.76	11.76	14.59	15.07	17.20	17.32
CaO	23.12	22.91	22.90	22.65	22.67	22.90
H_2O*	1.89	1.89	1.87	1.87	1.86	1.86
Total	98.20	99.60	99.16	101.25	98.53	100.28
Si	3.03	3.04	2.99	3.03	3.04	3.02
Al	2.33	2.31	2.15	2.16	1.91	1.96
Fe	0.65	0.70	0.88	0.89	1.06	1.05
Ca	1.99	1.95	1.98	1.92	1.99	1.97

* H_2O calculated on the basis of 1 H apfu.
† Calculated on the basis of 8 cations (excluding H).

CHEMICAL COMPOSITION

The crystals examined are homogeneous. Sector zoning was rarely observed. This zoning occurs in an hourglass fashion, the inner sector being richer in Fe. The crystal-chemical formulae (Table 5) obtained all show both Si and octahedral cations (Al+Fe) close to 3.0 apfu, thus suggesting the absence of any substitution involving the tetrahedral sites. One crystal was lost during polishing. The Fe contents obtained from EPMA agree with those deduced from XRD structural refinement (Fig. 1).

CRYSTAL CHEMISTRY

As previously observed (Gabe et al. 1973; Carbonin and Molin 1980; Bonazzi and Menchetti 1995), the structure responds to chemical variations both by adjusting polyhedral geometry (volume, distortion) and by twisting the linkage between polyhedra. Here we are concerned with the intracrystalline Fe distribution, and thus we focus on the variations involving the sites affected by the Al-Fe substitution. Crystal chemical features of the epidotes examined are compared with those of a set of natural crystals (Bonazzi and Menchetti 1995).

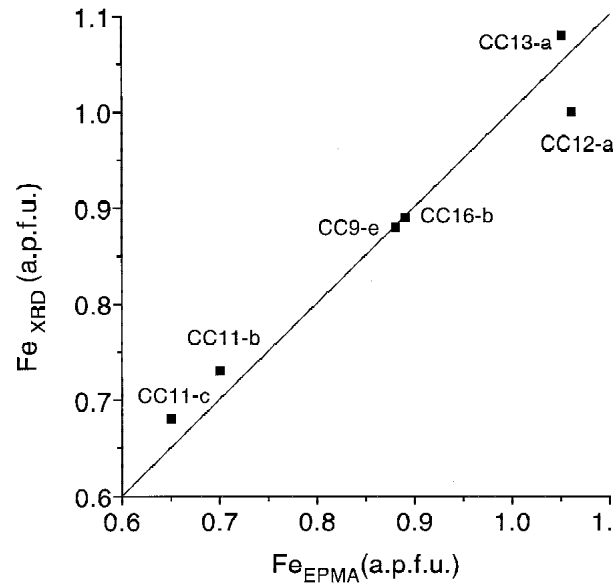

FIGURE 1. Fe contents of the crystals studied as obtained from EPMA and XRD single-crystal structure refinement respectively. The straight line has unit slope.

Fe-Al intracrystalline distribution

The refined octahedral occupancies (Table 6) show that crystals grown at 700 °C all have a small but significant amount of Fe located at the M2 site, whereas crystals grown at 600 °C do not. Fe partitioning between M3 and M1 sites (Fig. 2) for the crystals grown at 700 °C fit the 700 °C theoretical curve, even though M2 was not taken into consideration in this model. In contrast, crystals grown at 600 °C show a considerably higher disorder than expected. K_D values (=[Fe_{M1}][Al_{M3}]/[Fe_{M3}][Al_{M1}]) of the samples examined range from 0.033 to 0.054; comparing K_D values with those of natural samples (Bonazzi and Menchetti 1995) it can be observed that the latter show much greater order, the sample CZ (K_D = 0.027) being the only exception.

The M sites

The M sites are the most interesting part of the structure. They adjust their geometry in response to the chemical composition, and induce modifications in the surrounding structure accordingly. The most evident variations involve the <M-O> distances, which increase according to the Fe content of the site (Fig. 3). The distance of <M3-O> linearly increases with the number of electrons (ne^-) at this site: The synthetic samples match roughly the trend observed for the natural epidotes. The <M1-O> distances display similar trends (Fig. 3b), but are somewhat lower for the synthetic samples than for the natural ones. The difference is small when compared to the esd's; nevertheless it involves nearly all the samples and could be explained by the different degree of disorder between the two sets of epidotes. In fact, the M1 and M3 polyhedra share a common edge (O1-O4) whose length increases with the M3 dimensions. This edge, in turn, affects the size of the M1 octahedron. Therefore, the <M1-O> distance depends not only on the Fe content of the M1 site, but also on the M3 volume (i.e., by the Fe content of the M3 site). Thus, when comparing two samples with the same Fe_{M1}, the most disordered will have a smaller M3 and consequently a smaller M1 octahedron. This effect is relatively small if compared to the M1 volume increase caused by the Fe entry in M1, and therefore results only in subtle differences. When fitting <M1-O> vs. ne^-(M1) and ne^-(M3) for both natural and synthetic samples, we obtained the following regression line <M1-O> = 1.801(7) + 0.0064(7) ne^-(M1) + 0.0012(2) ne^-(M3) (r = 0.972).

The M2 site (Fig. 3e) is affected by a lesser substitution, and consequently is subject to minor geometrical changes. The <M2-O> distance varies from 1.882 to 1.891 Å in response to the entry of 0.08 Fe apfu.

TABLE 6. Refined Fe occupancies and *P-T* conditions of synthetic epidotes

Sample	T (°C)	P (kbar)	Fe_{M3}	Fe_{M1}	Fe_{M2}	Fe_{TOT}	K_D
CC11c	600	5.0	0.60 (1)	0.08 (1)	–	0.68	0.054
CC11b	600	5.0	0.65 (1)	0.08 (1)	–	0.73	0.049
CC9e	700	5.1	0.76 (1)	0.09 (1)	0.03 (1)	0.88	0.033
CC16b	700	5.3	0.76 (1)	0.10 (1)	0.03 (1)	0.89	0.036
CC20c	700	5.1	0.83 (1)	0.14 (1)	0.03 (1)	1.00	0.034
CC12a	700	4.6	0.81 (2)	0.13 (1)	0.06 (1)	1.00	0.036
CC13a	700	5.0	0.83 (1)	0.17 (1)	0.08 (1)	1.08	0.042

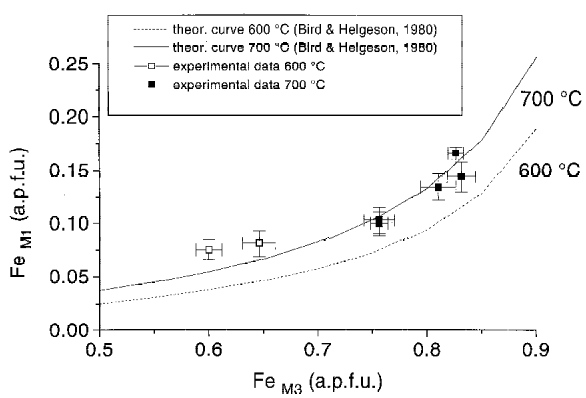

FIGURE 2. Fe occupancy of the M1 and M3 sites for the synthetic samples.

Unit-cell parameters

Unit-cell volume of epidotes is known to vary according to the chemical composition (Seki 1959; Myer 1965,1966; Gabe et al. 1973; Carbonin and Molin 1980; Bonazzi and Menchetti 1995). The *b* parameter increases markedly with the Fe content, whereas the *a* and *c* parameters increase slightly; the β angle in turn decreases somewhat. Although the synthetic and natural samples are characterized by very different degrees of Fe ordering, they both lie on the same trends of unit-cell parameters with Fe content (Fig. 4). This suggests that unit-cell volume is not affected by the Al-Fe intracrystalline distribution.

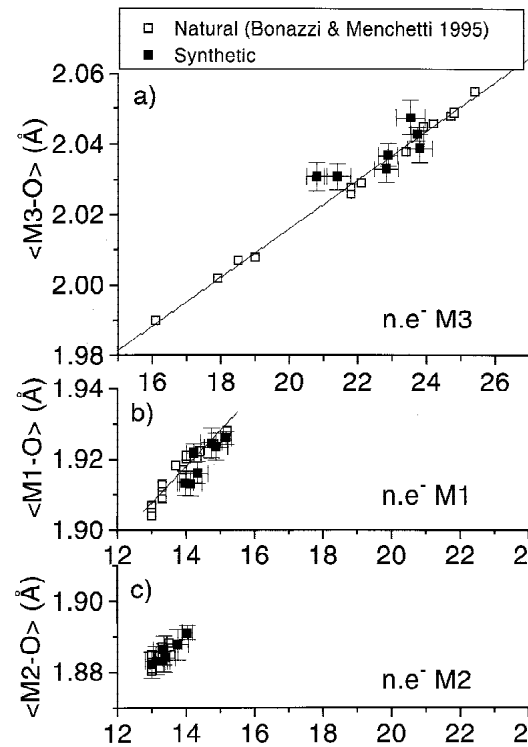

FIGURE 3. Mean octahedral M-O distances vs. the number of electrons at the site. **(a)** <M3-O> vs. ne^-(M3), regression line refers to the natural samples; **(b)** <M1-O> vs. ne^- (M1), regression line refers to natural samples; **(c)**; <M2-O> vs. ne^- (M2).

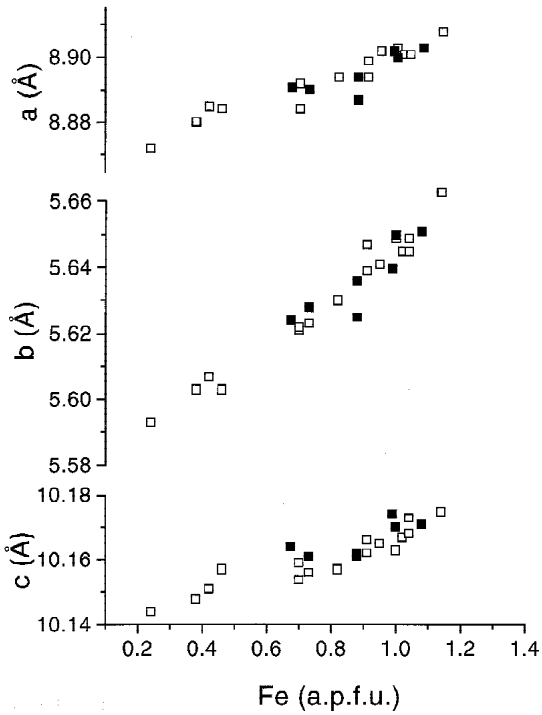

FIGURE 4. Unit-cell parameters vs. total Fe content. Filled symbols = synthetic samples of this study. Open symbols = natural samples of Bonazzi and Menchetti (1995).

DISCUSSION

The experimentally determined Fe intracrystalline distribution of the crystals always shows higher disorder than expected from the theoretical model by Bird and Helgeson (1980). Crystals synthesized at 600 °C have more Fe in the M1 site than predicted; crystals synthesized at 700 °C have Fe also in the M2 site, which was not taken into account in the model. The original experimental data of Dollase (1973), which were used in the theoretical model, represent a narrow compositional range; if we do not consider the presence of Fe in M2, the reported Fe distributions are not inconsistent with our data. The fact that Dollase (1973) did not find Fe in M2 may be due to difficulties in detecting small amounts of Fe_{M2} by means of Mössbauer spectroscopy. In fact, in the compositional range he examined, and considering the synthesis temperatures (from 620 to 686 ± 10 °C), Fe_{M2} likely does not exceed 0.03 apfu. Thus, our experimental data disagree to a lesser extent with the Mössbauer data of Dollase (1973), and to a larger extent with the theoretical Fe occupancies extrapolated for a wide compositional range.

Nonetheless, the presence of Fe in the M2 site complicates any attempt to model Fe disordering with temperature and requires more experimental data. However it should be noted that: (1) crystals formed at 600 °C (0.65–0.73 Fe apfu) do not have any Fe in M2; and (2) crystals formed at 700 °C (0.88–1.08 Fe apfu) have some Fe in the M2 site, its amount increasing with composition (from 0.03 to 0.08 apfu, respectively). The comparison suggests the existence of a region in the temperature-composition space where Fe enters also the M2 site, its amount increasing toward the high-temperature Fe-rich side.

The comparison of the crystal-chemical features of the crystals examined with those of a set of natural epidotes characterized by a much lower Fe disorder gives evidence on how disorder affects the structure. The differences observed are negligible: Fe disorder has little influence on the octahedral sites and, on the whole, it does not affect the unit-cell volume. This result is important when dealing with the pressure behavior of Fe disordering: In fact, if disordering were to be pressure-dependent, it would affect the unit-cell volume. The fact that it does not rules out any pressure dependency.

ACKNOWLEDGMENTS

Synthesis experiments were done at the Bayerisches Geoinstitut thanks to the EC "Human and Capital Mobility–Access to Large Scale Facility" program (contract no. ERBCHGECT940053 to D.C. Rubie). The Consiglio Nazionale delle Ricerche and MURST (grant 40%) are acknowledged for financial support to this research. We are grateful to Johanna Kruger who checked the original manuscript for its readability.

REFERENCES CITED

Bence, A.E. and Albee, A.L. (1968) Empirical correction factors for the electron microanalysis of silicates and oxides. Journal of Geology, 76, 382–402.

Bird, D.K. and Helgeson, H.C. (1980) Chemical interaction of aqueous solutions with epidote-feldspar mineral assemblages in geologic systems, I: thermodynamic analysis of phase relations in the system CaO-FeO-Fe_2O_3-Al_2O_3-SiO_2-H_2O-CO_2. American Journal of Science, 280, 907–941.

Bird, D.K., Cho, M., Janik, C.J., Liou, J.G., and Caruso, L.J. (1988) Compositional, order-disorder, and stable isotopic characteristics of Al-Fe epidote, state 2–14 drill hole, Salton Sea geothermal system. Journal of Geophysical Research, 93(B11), 13135-13144.

Bonazzi, P. and Menchetti, S. (1995) Monoclinic members of the epidote group: effects of the $Al \leftrightarrow Fe^{3+} \leftrightarrow Fe^{2+}$ substitution and of the entry of REE3+. Mineralogy and Petrology, 53, 133–153.

Carbonin, S. and Molin, G. (1980) Crystal-chemical considerations on eight metamorphic epidotes. Neues Jahrbuch für Mineralogie (Abhandlungen), 139, 205–215.

Dollase, W.A. (1973) Mössbauer spectra and iron distribution in the epidote-group minerals. Zeitschrift für Kristallographie, 138, 41–63.

Eugster, H.P. and Wones, D.R. (1962) Stability relations of the ferroginous biotite, annite. Journal of Petrology, 3, 82–125.

Fehr, K.T. and Heuss-Assblichler, S. (1997) Intracrystalline equilibria and immiscibility along the join clinozoisite-epidote: an experimental and ^{57}Fe study. Neues Jahrbuch für Mineralogie (Abhandlungen), 172, 43–67.

Gabe, E.J., Portheine, J.C., and Whitlow, S.H. (1973) A reinvestigation of the epidote structure: confirmation of the iron location. American Mineralogist, 58, 218–223.

Holdaway, M.J. (1972) Thermal stability of Al-Fe epidotes as a function of f_{O_2} and Fe content. Contribution to Mineralogy and Petrology, 37, 307–340.

Liou, J.G. (1973) Synthesis and stability relations of epidote, $Ca_2Al_2FeSi_3O_{12}(OH)$. Journal of Petrology, 14, 381–413.

Myer, G.H. (1965) X-ray determinative curve for epidote. American Journal of Science, 263, 78–86.

——— (1966) New data on zoisite and epidote. American Journal of Science, 264, 364–385.

North, A.C.T., Philips, D.C., and Mathews, F.S. (1968) A semiempirical method of absorption correction. Acta Crystallographica, A24, 351–359.

Patrier, P., Beaufort, D., Meunier, A., Eymery, J.P., and Petit S. (1991) Determination of the nonequilibrium ordering state in epidote from the ancient geothermal field of S. Martin: application of Mössbauer spectroscopy. American Mineralogist, 76, 602–610.

Sheldrick, G.M. (1976) SHEL-X program for structure determination. University of Cambridge, England.

Seki, Y. (1959) Relations between chemical composition and lattice constants of epidote. American Mineralogist, 44, 720–730.

MANUSCRIPT RECEIVED JUNE 23, 1998
MANUSCRIPT ACCEPTED DECEMBER 10, 1998
PAPER HANDLED BY JAMES W. DOWNS